

38. PALEOCEANOGRAPHY OF THE WESTERN MEDITERRANEAN DURING THE PLEISTOCENE: OXYGEN AND CARBON ISOTOPE RECORDS AT SITE 975¹

Catherine Pierre,² Paul Belanger,³ Jean François Saliège,² Marie José Urrutiaguer,² and Anne Murat⁴

ABSTRACT

The Quaternary sedimentary sequence retrieved at Site 975, on the Menorca Rise in the West Balearic Basin, contains 36 sapropel layers that are considered to have been deposited under environmental conditions similar to those of the eastern Mediterranean sapropels. The oxygen and carbon isotope records of the planktonic foraminifer *Globigerina bulloides* are used to establish the precise chronology of the sapropel events in this part of the western Mediterranean as well as for paleoceanographic reconstructions.

Three major breaks at 1.7 Ma, 0.9 Ma, and 0.42 Ma are well identified in the $\delta^{18}\text{O}$ record of Site 975. The lower event occurs above the Pliocene/Pleistocene boundary (1.83 Ma), while the other two younger events are approximately coincidental with the major augmentation events of the Northern Hemisphere ice sheets. The 1.9-m.y.-long $\delta^{18}\text{O}$ record in the West Balearic Basin follows a pattern similar to that found in the open ocean; however, the signal is amplified because of restrictions in circulation between the Mediterranean and the Atlantic. The amplification of the glacial-interglacial oscillations was particularly significant in the upper Pleistocene. After 0.42 Ma, compared to the previous period, the increase by 1‰ of the $\delta^{18}\text{O}$ values during glacial stages was caused both by surface waters cooling and by excess evaporation increasing over freshwater input, thereby inducing increased surface salinities.

The $\delta^{13}\text{C}$ variations of *G. bulloides* at Site 975 reflect both the global ocean and local Mediterranean $\delta^{13}\text{C}$ variations in surface waters. During the Quaternary in the West Balearic Basin, the surface productivity levels were not only controlled by the climate evolution but also by the thermohaline stratification.

The sapropels were principally deposited within interglacial stages, at times of the maximum values of the insolation cycles, when surface productivity is also interpreted to be high. The random distribution of sapropels in the western Mediterranean throughout the last 1.9-m.y. period indicates that these depositional events were not caused by regular climatic processes. Furthermore, a few sapropel layers from the eastern Mediterranean as well as from the other western Mediterranean basins have no equivalent in the West Balearic Basin, meaning that the hydrological and climatic controls on the export production budget were not uniform within the Mediterranean.

INTRODUCTION

The main objectives of the Ocean Drilling Program (ODP) Legs 160 and 161 in the Mediterranean were to study the entire Pliocene–Quaternary sedimentary sequence to establish both the chronology of the sapropels and the associated changes in the hydrology and productivity of the area. The primary source of these data comes from the various records of micropaleontological and geochemical proxies from planktonic foraminifers. A synthesis paper compiling and studying the results of the different teams involved in this research program can be found in the synthesis section (Comas et al., Chap. 44, this volume).

The current opinion is that sapropels were deposited under anoxic bottom conditions during periods of enhanced rates of biological productivity. Murat (Chap. 41, this volume) summarizes paleoceanographic models that have been proposed for sapropel formation: (1) an increased stratification of lower salinity surface water resulting in reduced circulation of bottom water; or (2) a combination of a more thinly stratified surface layer preventing bottom-water circulation, and a shallower pycnocline within the photic zone causing increased productivity and greater accumulation of organic matter on the seafloor creating these sapropels. Furthermore, sapropel deposition does

not seem to require a characteristic climate because it might occur during full interglacial or interstadial times or sometimes during full-glacial periods. Wetter conditions, however, are interpreted to be a constant climatic constraint, possibly linked to precession minima and maximum insolation resulting in an increased intensity in the African-Asian monsoon system (Hilgen, 1991).

The continuous sedimentary records that were recovered during Legs 160 and 161 have shown that sapropels started to be deposited during the early Pliocene in the eastern Mediterranean and during the latest Pliocene in the western Mediterranean. In the eastern Mediterranean, a maximum of 80 sapropel units have been recognized, with a maximum of 45 of these units deposited during the Quaternary. The total organic carbon (TOC) content in the eastern Mediterranean sapropels may be as high as 30%. In the western Mediterranean, a maximum total of 68 sapropels have been recognized at Site 979 in the Alboran basin; their TOC content ranges from 0.8% to 6.4%, the highest values having been measured in the Tyrrhenian Basin (Emeis, Robertson, Richter, et al., 1996; Comas, Zahn, Klaus, et al., 1996; Murat, Chap. 41, this volume).

The goal of this paper is to present the oxygen and carbon isotope records in planktonic foraminifers at Site 975 to establish the chronological framework of the sapropels and to propose paleoceanographic reconstructions during the Pleistocene–Holocene in this part of the western Mediterranean.

SITE 975

ODP Site 975 is located on the Menorca Rise, between the South Balearic Basin and the Algerian Basin (38°53.8'N, 4°30.6'E). Pliocene–Pleistocene sediments were continuously cored in 2415 m

¹Zahn, R., Comas, M.C., and Klaus, A. (Eds.), 1999. *Proc. ODP, Sci. Results*, 161: College Station, TX (Ocean Drilling Program).

²UMR 7617, CNRS-ORSTOM-UPMC, Laboratoire d'Océanographie Dynamique et de Climatologie, Université Pierre et Marie Curie, 4 Place Jussieu, 75252 Paris Cedex 05, France. Pierre: cat@lodyc.jussieu.fr

³Department of Geological Sciences, University of Oregon, Eugene, OR 97403-1272, U.S.A. (Present address: 4429 Valerie St., Bellaire, TX 77401-5626, U.S.A.)

⁴Intechmer, BP 324, 50103 Cherbourg Cedex, France.

water depth, and 317 and 313 m were recovered in Holes 975B and 975C, respectively. Coring stopped within the upper Messinian (Miocene) evaporites. The Pliocene/Pleistocene boundary was recognized in Core 13H of Hole 975B, at about 115 meters below seafloor (mbsf). The average sedimentation rate at Site 975 is estimated to be 6.8 cm/m.y. for the Holocene–Pleistocene, or about twice the sedimentation rate calculated at Site 974 in the Tyrrhenian Basin, and at Sites 967 and 964 in the Levantine and Ionian Basins. The sedimentation rate at Site 975, however, is only about one-third of the sedimentation rate of the Alboran Basin Sites 976–979 (Emeis, Robertson, Richter, et al., 1996; Comas, Zahn, Klaus, et al., 1996).

Sediments consist basically of nannofossil clay, nannofossil ooze and calcareous silty-clay. The sapropels, whose thickness ranges between 1 and 13 cm, have TOC contents between 0.84% and 2.9% (Table 1). This means that conditions favoring the deposition of sapropels were stable over a period of about 150 to 1500 years, if a constant sedimentation rate is assumed.

METHODS

The samples were taken in Hole 975B at regular 20-cm intervals from the top of Core 161-975B-1H down to 14H to encompass the Pliocene/Pleistocene boundary; a few disturbed portions of the cores were replaced by their depth-equivalent sections in Hole 975C. The entire data set, in which most, although not all, sapropels were sampled, represents 630 levels (Table 2 on CD-ROM, back pocket, this volume). The sampling resolution is about 3 k.y., which is high enough to recognize the Milankovitch orbital cycles. The depth of samples was adjusted to that of meters composite depth (mcd) according to the shipboard observations (Comas, Zahn, Klaus, et al., 1996).

Stable isotope analyses were performed on the planktonic foraminifer *Globigerina bulloides*, a species which has its maximum development in late spring when the seasonal thermocline begins to be established (Pujol and Vergnaud-Grazzini, 1995).

The upper part of the series down to 31.85 mcd (Sample 161-975B-4H-4, 140–142 cm) was analyzed in the isotope laboratory of Dr. Rob Dunbar at Rice University, Houston, TX, USA. Approximately 10 cm³ samples were dried in an oven at 60°C. Samples were then weighed, soaked in a 5% Calgon solution for a few hours, washed on a 63- μ m sieve, filtered, and dried. *G. bulloides* were then selected from the 250- to 355- μ m size fraction for analyses. Before isotopic analysis, the picked *G. bulloides* foraminifers were cleaned in an ultrasonic bath to remove fine-fraction contamination. Roasting of samples before analysis was not performed or deemed necessary to remove volatile organics. Generally, between 25 to 35 foraminifers were used for each individual analysis. These carbonate samples were dissolved in 100% phosphoric acid at 50°C. Resulting CO₂ and H₂O were separated by a series of three freezing/transfer steps. The purified CO₂ was analyzed in an on-line VG Micromass 602D mass spectrometer. Isotopic results are referred to Peedee belemnite (PDB) in the standard δ notation (Craig, 1957). Calibration to PDB was achieved through intercalibration of three intermediate standards. Agreement among all standards was $\pm 0.05\%$. Analytical precision of carbonate standards run before and after each analytical session was ± 0.11 (1 σ) for $\delta^{18}\text{O}$ and ± 0.09 (1 σ) for $\delta^{13}\text{C}$ values. Replicates were run on about 14% of the samples. Analytical precision for foraminiferal replicates was about 0.09 for $\delta^{18}\text{O}$ and about 0.12 for $\delta^{13}\text{C}$.

The lower part of the series down to 137.45 mcd (Sample 161-975B-14H-6, 130–132 cm) was studied in the Laboratoire d'Océanographie Dynamique et de Climatologie (LODYC) at the Pierre and Marie Curie University, Paris, France. An average number of 10 to 12 individuals of each species was picked in the 250- to 355- μ m frac-

Table 1. Depth position, position on the oxygen isotopic curve, and extrapolated ages of the sapropel layers at Site 975.

Sapropel	TOC (%)	Depth top (mcd)	Depth bottom (mcd)	Age top (ka)	Age bottom (ka)	Duration (k.y.)	Insolation cycle	Isotopic stage
501	1.54	9.65	9.76	122.18	122.82	0.64	12	5.5
502	1.10	15.37	15.415	163.22	163.78	0.56	?	6.5
503	1.15	15.81	15.91	168.65	169.89	1.23	16	6.5
504	1.66	16.00	16.02	171.00	171.23	0.23	16	6.5
505	1.52	16.40	16.43	175.62	175.96	0.35	16	6.5
506	1.72	17.72	17.80	193.84	195.83	1.99	18	7.1
507	0.92	20.20	20.25	237.81	238.49	0.68	22	7.5
508	0.97	27.94	28.01	331.03	331.25	0.22	30	9.3
509	1.42	35.46	35.47	405.00	405.10	0.10	38	11.3
510	0.89	40.48	40.52	464.66	465.26	0.60	44	12.3
511	1.90	43.51	43.58	481.00	482.00	1.00	46	13.11
512	1.36	47.22	47.35	524.33	526.47	2.14	50	13.3
513	1.09	49.50	49.53	574.00	574.55	0.55	54	15.1
514	2.90	50.77	50.87	596.47	598.18	1.71	56	15.3
515	1.54	51.79	51.83	613.92	614.60	0.68	58	15.5
516	1.61	51.94	52.03	616.49	617.54	1.05	58	15.5
517	1.10	54.70	54.75	643.48	643.85	0.37	60	16.3
518	0.95	61.51	61.55	731.88	732.51	0.64	68	18.3
519	2.20	73.24	73.26	907.75	908.02	0.27	86	23
520	1.47	76.72	76.82	949.20	950.62	1.42	90	25
521	1.00	77.12	77.17	956.78	957.81	1.03	90	25
522	1.00	78.32	78.36	978.28	978.94	0.66	92	27
523	2.59	79.60	79.66	999.52	1000.52	1.00	94	27
524	1.33	81.06	81.14	1027.60	1028.67	1.07	96	29
525	2.69	83.74	83.82	1072.44	1073.98	1.54	100	31
526	1.06	84.73	84.74	1091.53	1091.72	0.19	102	31
527	1.38	85.63	85.65	1112.75	1113.13	0.38	104	33
528	2.02	90.65	90.67	1184.88	1185.22	0.34	112	35
529	1.99	92.77	92.80	1221.44	1221.78	0.33	116	37
530	1.08	101.52	101.55	1332.20	1332.60	0.41	128	41
531	1.59	105.93	105.95	1398.47	1398.79	0.32	134	45
532	0.84	106.63	106.65	1409.53	1409.84	0.32	136	46
533	0.99	113.02	113.11	1524.19	1525.05	0.86	148	51
534	1.06	126.11	126.12	1714.95	1715.08	0.13	168	60?
535	1.11	127.90	127.91	1737.79	1737.92	0.13	170	61
536	0.90	131.18	131.20	1807.61	1808.09	0.48	176	65

Notes: The sapropel numbers and TOC contents were obtained from the Leg 161 *Initial Reports* volume (Comas, Zahn, Klaus, et al., 1996) and Murat (Chap. 41, this volume). The insolation cycle numbering is based on the astronomical solution of Laskar (1990).

tion to obtain the weight of ~200 µg that is necessary for stable isotope analyses. All samples were roasted for 2 hr under vacuum at 350°C to remove any volatile organic component. This procedure was proved to be not fractionating since the carbonate decomposition begins at 500°C. The CO₂ was extracted from the carbonate of foraminifers at 90°C with 103% phosphoric acid on the automatic device, coupled with a triple collector Optima Isogas mass-spectrometer. With each twelve samples, two standard carbonates are included, giving a reproducibility of measurements made on the laboratory reference of ± 0.02‰ for both δ¹⁸O and δ¹³C values. The analytical precision was 0.01‰. Standard deviations of separated analyses of the same foraminiferal species were ± 0.10‰ for δ¹⁸O and ± 0.05‰ for δ¹³C.

Because of the different analytical procedures used in the two laboratories, interlaboratory calibration between Rice University and LODYC was performed using selected samples, to check the good adjustment of isotopic measurements. The main causes of isotopic fractionation should come either from the quality of the phosphoric acid or from the temperature stability during the acid attack.

All analytical data from Holes 975B and 975C have been listed and mixed to obtain a single record of the oxygen and carbon isotope variations with depth (Table 2 on CD-ROM, back pocket, this volume).

THE OXYGEN ISOTOPE RECORD AT SITE 975

The oxygen isotope stratigraphy from the Holocene to the upper Pliocene at Site 975 is based on the continuous record of *G. bulloides* allowing the identification of Isotopic Stages 1 to 69. The time-scale calibration of the oxygen isotopic stages corresponds to the orbitally derived time scales of Shackleton et al. (1990), Bassinot et al. (1994), Tiedemann et al. (1994), and Lourens et al. (1996). The age control points of the isotopic events used for this calibration are listed in Table 3. Linear interpolation was applied between two adjacent age control points, assuming a constant sedimentation rate within this time interval. The chronologies deduced from the oxygen isotope stratigraphy and from the nannofossil biostratigraphy (de Kaenel et al., Chap. 13, this volume) were carefully compared to correlate the two time scales.

The δ¹⁸O record of *G. bulloides* is shown as a function of depth (Fig. 1A) and as a function of age (Fig. 1B). Four major intervals can be recognized, based on the amplitude of the isotopic oscillations between glacial and interglacial stages and on the frequency of the glacial periodicity. The detailed δ¹⁸O-age records and the location of the sapropels are reported in Figure 2A–C. Table 1 gives the age estimations and location of sapropels for the oxygen isotope curve.

Interval I: Holocene–Upper Pleistocene (0–37 mcd, 0–0.42 Ma)

Interval I, isotopic stages 1 to 11, corresponds to the Holocene–upper Pleistocene period and has a very high δ¹⁸O amplitude (average 2.9‰). All isotopic stages and substages are recognized, with the shape of the peaks similar to those of the classical standard curve of Prell et al. (1986). The average maximum and minimum δ¹⁸O values reach 3.5‰ and 0.6‰, respectively. The periodicity of the isotopic oscillations is typically that of eccentricity (i.e., 100 k.y. cycle), as is also evidenced by the data from Sites 976 and 977 (von Grafenstein et al., Chap. 37, this volume).

Nine sapropels are present in this interval. Although sapropels 501, 502, 503, 504, and 505 were not sampled, their age was estimated from their depth position, and they are tentatively located on the oxygen isotope curve (Fig. 2A; Table 1). The sapropels of interval I occur in isotopic levels 5.5, 6.5, 7.1, 7.5, 9.3, and 11.3 (i.e., during warmer climatic episodes).

Table 3. Age control points used for the age extrapolation at Site 975.

Depth (mcd)	Age (ka)	Isotopic stage
1.18	19	2.2
2.65	30	3.1
4.46	52	3.3
5.17	65	4.2
6.45	80	5.1
6.75	86	5.2
8.18	99	5.3
9.62	122	5.5
11.84	135	6.2
14.38	151	6.4
16	171	6.5
17.04	183	6.6
17.73	194	7.1
18.57	216	7.3
19.68	228	7.4
20.21	238	7.5
21.11	249	8.2
22.85	269	8.4
27.93	331	9.3
30.48	339	10.2
32.65	368	11.1
35.46	405	11.3
38.45	434	12.2
40.9	471	12.4
43.51	481	13.1
45.75	513	13.2
47.2	524	13.3
48.05	538	14.2
49.5	574	15.1
50.1	585	15.2
51.97	617	15.5
53.2	628	16.2
54	631	16.23
54.5	642	16.3
57.75	666	17.1
59.15	688	17.3
60.55	720	18.23
61.52	732	18.3
62.57	750	18.4
64.52	782	19.3
66.12	798	20.23
69.51	837	21
70.75	882	22
73.11	906	23
74	918	24
76.79	950	25
77.52	965	26
79.93	1005	28
81.08	1028	29
82.51	1044	30
83.51	1068	31
84.91	1095	32
85.64	1113	33
86.73	1127	34
89.3	1169	35
90.66	1185	35
91.47	1203	36
92.64	1220	37
94.98	1246	38
98.55	1292	40
102.54	1346	42
104.95	1383	44
107.04	1416	46
109.04	1462	48
111.6	1505	50
113	1524	51
115	1543	52
117.14	1563	53
117.94	1574	54
120.7	1625	56
122.95	1656	58
125.33	1705	60
128.7	1748	62
130.4	1789	64
132.37	1836	66
134.97	1868	68
135.17	1899	69

Interval II: Middle Pleistocene–Upper Lower Pleistocene (37–72 mcd, 0.42–0.9 Ma)

In interval II, between isotopic stages 12 and 22, the amplitude of δ¹⁸O variations decreases to 1.9‰; it includes the middle Pleistocene and the upper part of the lower Pleistocene. Again, all the isotopic stages are well recorded at Site 975. The average maximum and min-

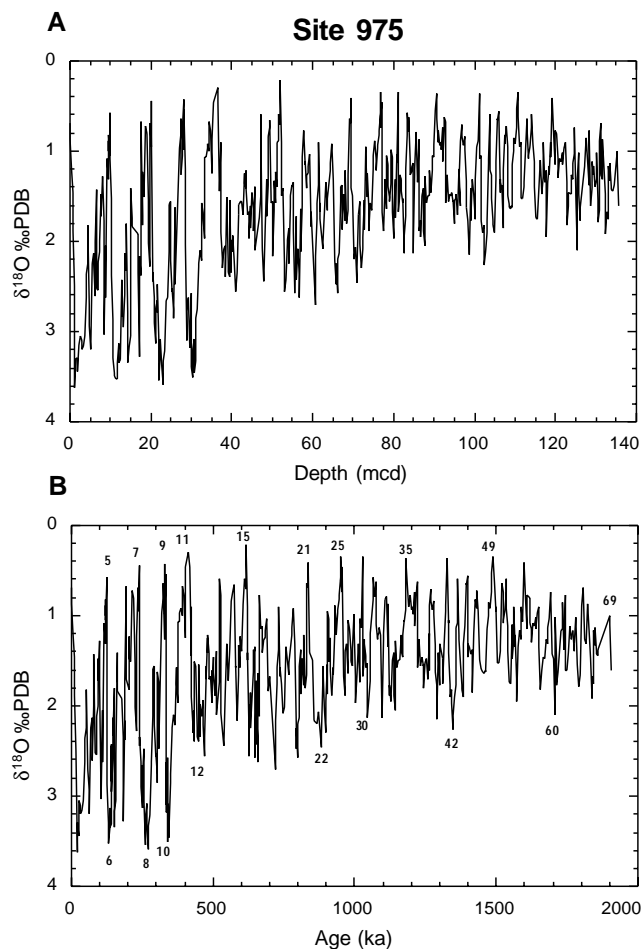


Figure 1. **A.** The $\delta^{18}\text{O}$ record of *Globigerina bulloides* as a function of depth (mcd) at Site 975. **B.** The $\delta^{18}\text{O}$ record of *Globigerina bulloides* as a function of interpolated age (ka) at Site 975. Numbers indicate isotopic stages.

imum $\delta^{18}\text{O}$ values reach 2.5‰ and 0.6‰, respectively. The periodicity of the isotopic oscillations remains that of the eccentricity controlled 100 m.y. cycles in this interval.

The nine sapropels present in this interval have all been sampled. They occur in isotopic levels 12, 13.11, 13.3, 15.1, 15.3, 15.5, 16.3 and 18.3 (Fig. 2B; Table 1). These sapropels were deposited during warmer climatic episodes, mostly during interglacial stages. Two exceptions, sapropels 510 and 517, were deposited during warmer episodes of glacial stages 12 and 16.

**Interval III: Lower Pleistocene
(72–127 mcd, 0.9–1.7 Ma)**

In interval III, between isotopic stages 23 and 60, the amplitude of $\delta^{18}\text{O}$ variations decreases slightly to 1.6‰; this is because of a slight decrease of the maximum and minimum $\delta^{18}\text{O}$ values, which average 2.1‰ and 0.5‰, respectively. The periodicity of the glacial-interglacial cycles becomes that of the obliquity at 40 m.y.

Fifteen sapropels are present in this interval. They are located in isotopic stages 23, 25, 27, 29, 31, 33, 35, 37, 41, 45, and 51 on the isotopic curve (i.e., again during warm interglacial episodes Fig. 2C; Table 1).

**Interval IV: Lowermost Pleistocene–Uppermost Pliocene
(127–136 mcd, 1.7–1.9 Ma)**

The upper limit of interval IV corresponds to isotopic stage 61; isotopic stage 69 was identified at the base of the sampled section.

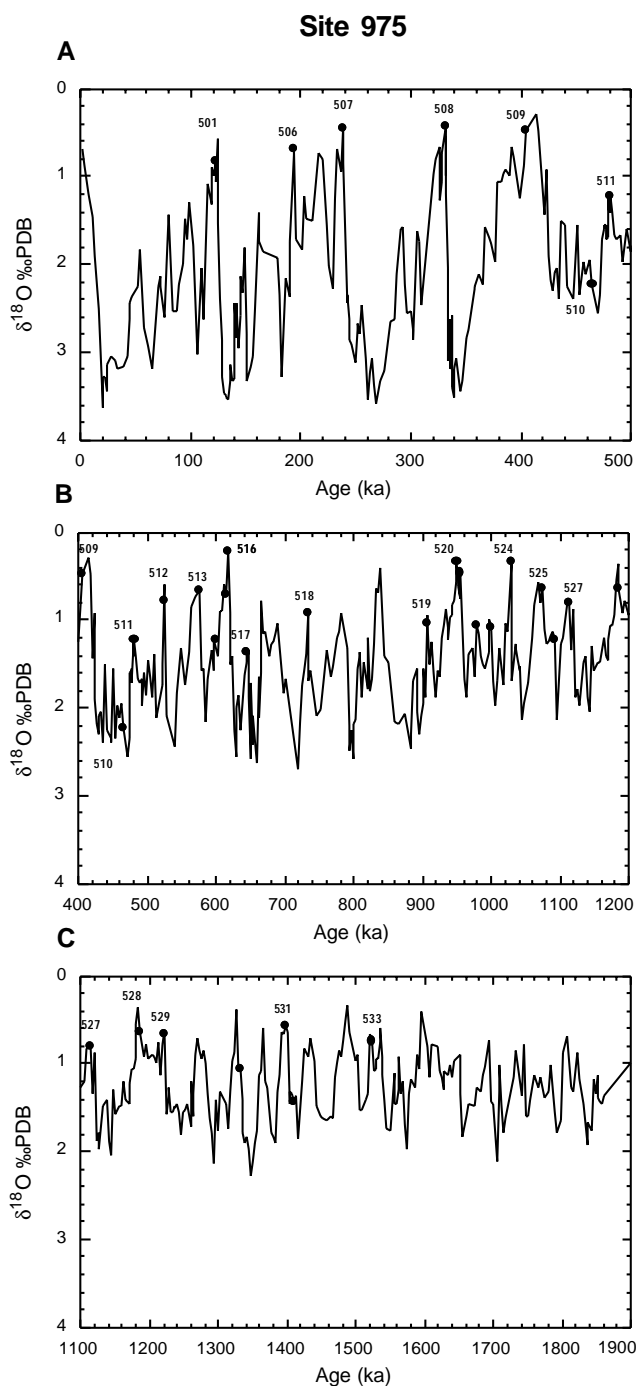


Figure 2. **A.** The $\delta^{18}\text{O}$ record of *Globigerina bulloides* during the period 0–500 ka. The δ values measured in the sapropel layers are marked by the solid circles. The sapropel numbers are those given in the Leg 161 *Initial Reports* (Comas, Zahn, Klaus, et al., 1996). **B.** The $\delta^{18}\text{O}$ record of *Globigerina bulloides* during the period 400–1200 ka. **C.** The $\delta^{18}\text{O}$ record of *Globigerina bulloides* during the period 1100–2000 ka.

The Pliocene/Pleistocene boundary is placed at 1.83 Ma, and thus is included within interval IV. This interval is characterized by the small amplitude (1.0‰) of the $\delta^{18}\text{O}$ variations, which is caused mostly by a weak decrease by 0.3‰ of the maximum $\delta^{18}\text{O}$ values (averaging 1.8‰) and by a weak increase by 0.3‰ of the minimum $\delta^{18}\text{O}$ values (averaging 0.8‰).

The three sapropels within this interval (534, 535, and 536) correspond to the deepest layers at Site 975. They were not sampled, but

their age estimations deduced from their depth position indicate that they were deposited at the onset of Pleistocene during the interglacial isotopic stages 61 and 65 (Fig. 2C; Table 1).

THE CARBON ISOTOPE RECORD AT SITE 975

The $\delta^{13}\text{C}$ record of *G. bulloides* at Site 975 is shown as a function of depth (Fig. 3A) and as a function of age (Fig. 3B). Detailed $\delta^{13}\text{C}$ -age records with the location of sapropels are also represented in Figure 4A–C.

The carbon isotope variability throughout the Pleistocene, although somewhat noisy, exhibits positive and negative peaks that can be roughly correlated with the oxygen isotope stages (Fig. 3A, B). The highest $\delta^{13}\text{C}$ values are generally coeval with the highest $\delta^{18}\text{O}$ values of the glacial stages, and the lowest $\delta^{13}\text{C}$ values are coeval with the lowest $\delta^{18}\text{O}$ values of the interglacial stages. This means that surface productivity was higher during glacial times than during interglacial times, a conclusion which has been already verified in the global ocean as well as in the Tyrrhenian Basin (Vergnaud-Grazzini et al., 1990). However, looking in more detail, the covariation of $\delta^{18}\text{O}$ and $\delta^{13}\text{C}$ values at Site 975 is not fully verified for the entire Quaternary, meaning that a local Mediterranean overprint is superimposed on the global signal.

Four intervals may be distinguished by their mode and amplitude of $\delta^{13}\text{C}$ variations; their age boundaries match well with those defined from the oxygen isotope curve.

Interval I: Holocene–Upper Pleistocene (0–37 mcd, 0–0.42 Ma)

The $\delta^{13}\text{C}$ values oscillate between -0.15‰ and -1.35‰ throughout the Holocene–upper Pleistocene period, giving a maximum amplitude of 1.2‰ for the $\delta^{13}\text{C}$ variations (Fig. 4A). The $\delta^{13}\text{C}$ values measured in the sapropels are low (-1.55‰ to -1.17‰), except in sapropel 506 where the value is moderately low (-0.5‰).

Interval II: Middle Pleistocene–Upper Lower Pleistocene (37–72 mcd, 0.42–0.9 Ma)

Before 0.42 Ma and down to 0.9 Ma, the maximum amplitude of $\delta^{13}\text{C}$ variations reached 1.6‰ , the $\delta^{13}\text{C}$ values displaying regular oscillations between 0.1‰ and -1.5‰ (Fig. 4B). In this evolution, most of the lowest $\delta^{13}\text{C}$ values are attributed to the sapropel occurrences.

Interval III: Lower Pleistocene (72–127 mcd, 0.9–1.7 Ma)

During the lower Pleistocene, the amplitude of $\delta^{13}\text{C}$ variations decreased to about 1.3‰ , and the maximum and minimum $\delta^{13}\text{C}$ values increased progressively by about 1.0‰ throughout the whole period (Fig. 4C). This increase, as well as the increasing trend in the total carbonate content (Comas, Zahn, Klaus, et al., 1996), indicates a major change toward a more productive regime in the surface waters. A similar behavior was observed at ODP Site 653 in the Tyrrhenian Basin for the same time interval (Vergnaud-Grazzini et al., 1990). The $\delta^{13}\text{C}$ values recorded in the sapropels within this time interval correspond mostly to the lowest values of the oscillations.

Interval IV: Lowermost Pleistocene–Uppermost Pliocene (127–136 mcd, 1.7–1.9 Ma)

The amplitude of the $\delta^{13}\text{C}$ oscillations remained at the level of 1.3‰ in the lowermost Pleistocene, but it decreased slightly below the Pliocene/Pleistocene boundary where the maximum and minimum $\delta^{13}\text{C}$ values became stable at 0.5‰ and -0.4‰ , respectively (Fig. 4C).

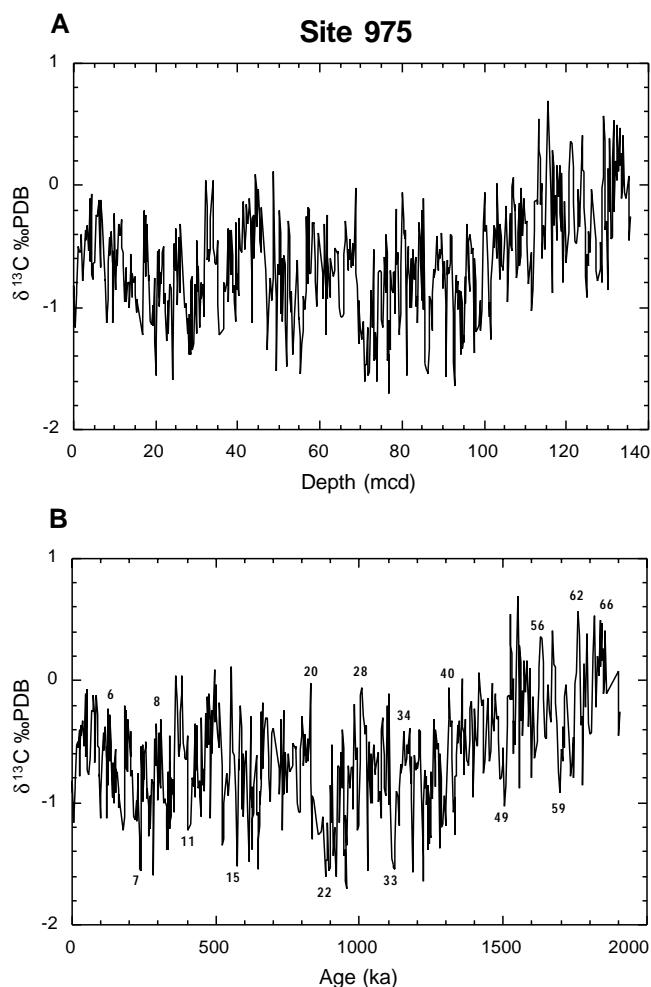


Figure 3. A. The $\delta^{13}\text{C}$ record of *Globigerina bulloides* as a function of depth (mcd) at Site 975. B. The $\delta^{13}\text{C}$ record of *Globigerina bulloides* as a function of interpolated age (ka) at Site 975. Numbers indicate isotopic stages.

DISCUSSION

At Site 975, the amplitude of the $\delta^{18}\text{O}$ oscillations increased by steps from the uppermost Pliocene up to Holocene, from about 1.0‰ prior to 1.7 Ma, to 1.6‰ between 1.7 Ma and 0.9 Ma, to 1.9‰ between 0.9 Ma and 0.42 Ma, to reach 2.9‰ during the upper Pleistocene. Synchronous shifts, but of less amplitudes, were also observed at Sites 976 and 977 in the Alboran Basin (von Grafenstein et al., Chap. 37, this volume) and at Site 653 in the Tyrrhenian Basin (Vergnaud-Grazzini et al., 1990). Outside the Mediterranean, the $\delta^{18}\text{O}$ variation by about 1.2‰ records the cyclic changing of ice volume in the Northern Hemisphere during glacial and interglacial periods (Fairbanks, 1989). Superimposed on this global ice effect, the additional $\delta^{18}\text{O}$ changes in the foraminifer records are a result of either thermal effects with 1°C cooling resulting in a $\delta^{18}\text{O}$ increase by 0.24‰ (Craig, 1965) or to local variations in the freshwater budget. For instance, in the modern Mediterranean, an increase by 1‰ of the surface water $\delta^{18}\text{O}$ values corresponds to a 4‰ increase of the salinity (Pierre, in press).

In the West Balearic Basin, the global increase of the amplitude of the $\delta^{18}\text{O}$ oscillations from the uppermost Pliocene up to the Holocene was caused by a multi-step drift by 1.7‰ of the glacial $\delta^{18}\text{O}$ values, that registers the effects of major climatic or hydrological changes (Fig. 1A, B). In the other parts of the western Mediterranean, a similar drift is observed in the glacial $\delta^{18}\text{O}$ values but it is only of

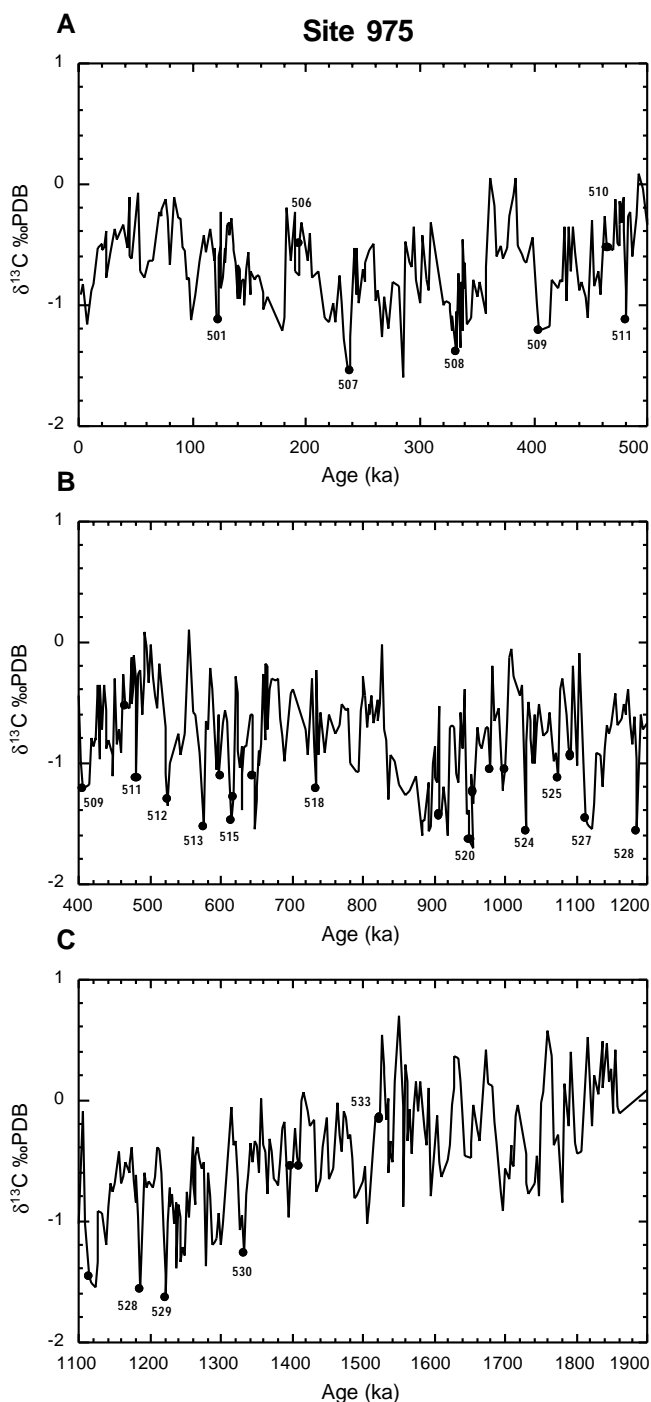


Figure 4. A. The $\delta^{13}\text{C}$ record of *Globigerina bulloides* during the period 0–500 ka. The δ values measured in the sapropel layers are marked by the filled circles. The sapropel numbers are those given in the Leg 161 *Initial Reports* (Comas, Zahn, Klaus, et al., 1996). B. The $\delta^{13}\text{C}$ record of *Globigerina bulloides* during the period 400–1200 ka. C. The $\delta^{13}\text{C}$ record of *Globigerina bulloides* during the period 1100–2000 ka.

1.0‰ in the Alboran Basin (von Grafenstein et al., Chap. 37, this volume) and in the Tyrrhenian Basin (Vergnaud-Grazzini et al., 1990). This indicates that the climatic and hydrological changes during the Pleistocene were not exactly similar within the western Mediterranean.

At about 1.7 Ma, the glacial $\delta^{18}\text{O}$ values increased by 0.3‰ and the interglacial $\delta^{18}\text{O}$ values decreased by 0.3 at Site 975. These variations are thought to register weak climatic changes toward dryer/cooler glacial stages, and wetter/warmer interglacial stages at the onset of Pleistocene.

Near 0.9 Ma, the glacial $\delta^{18}\text{O}$ values were again shifted by 0.4‰ while the interglacial values remained at similar levels. This shift is also recorded in the Alboran Basin at Sites 976 and 977 with a similar amplitude, while it appears weaker at Site 653 in the Tyrrhenian Basin. Converting the $\delta^{18}\text{O}$ variation to temperature variation indicates that, in the period 0.42–0.9 Ma, the surface temperatures during glacial stages were lower by 2°C compared to those during the glacial stages before 0.9 Ma. Alternatively, this variation might be caused by higher rates of evaporation, in turn a result of increasing dryness in the glacial Mediterranean area.

After 0.42 Ma, the $\delta^{18}\text{O}$ values of *G. bulloides* at Site 975 were similar to those measured at Site 653 in the Tyrrhenian Basin (Vergnaud-Grazzini et al., 1990), except for the fact that they were more positive by about 0.5‰ than at Sites 976 and 977 in the Alboran Sea (von Grafenstein et al., Chap. 37, this volume). This may be fully explained by the $\delta^{18}\text{O}$ variability of the Mediterranean surface waters where *G. bulloides* precipitated their shells. In the modern Mediterranean, the $\delta^{18}\text{O}$ values of the surface waters in the Balearic Basin are enriched by about 0.4‰ to 0.5‰ relative to those from the Alboran Basin because of the increasing evaporation over the Mediterranean, an effect that is also responsible for the ~1.5‰ increase in surface-water salinity between the Alboran Basin and the Balearic Basin (Pierre, in press). The fact that the $\delta^{18}\text{O}$ gradient was similar to the present day during the upper Pleistocene means that at this time the surface salinity gradient between these parts of the western Mediterranean was not significantly different from today's salinity gradient. During this period, the glacial $\delta^{18}\text{O}$ values increased by 1.0‰ at Site 975, a value higher by 0.5‰ than at Sites 976 and 977 in the Alboran Basin (von Grafenstein et al., Chap. 37, this volume) and at Site 653 in the Tyrrhenian Basin (Vergnaud-Grazzini et al., 1990). The change by 0.5‰ may be attributed to cooler glacial conditions in the surface waters during the upper Pleistocene than before; a temperature decrease by about 2°C may thus be estimated between the middle and the upper Pleistocene. If we assume that the thermal response to the glacial conditions was rather uniform in the surface waters of the western Mediterranean, then the remaining 0.5‰ $\delta^{18}\text{O}$ variation at Site 975 has to be attributed to a local effect. It might have corresponded to an increased freshwater deficit in the West Balearic Basin during glacial times of the upper Pleistocene. Assuming that the slope between $\delta^{18}\text{O}$ and salinity was not different from the modern value of 0.25 (Pierre, in press), salinities of surface waters in the West Balearic Basin were thus higher by 2‰ during the glacial stages of the upper Pleistocene, compared to those during the glacial stages of the middle to lower Pleistocene. An alternative should be that before 0.42 Ma, the salinity gradient in the western Mediterranean was similar to the modern one but the glacial surface water temperatures were higher by 2°C in the West Balearic Basin compared to those of the Alboran and Tyrrhenian Basins.

During the whole Pleistocene, the amplitudes of the $\delta^{18}\text{O}$ oscillations became, thus, more and more higher in the Mediterranean compared to those of the open ocean, a characteristic of the restricted Mediterranean basin that amplified the global oceanic signal when the terms of the evaporation-precipitation budget were modified, even weakly. During the glacial stages, the increased dryness over the Mediterranean, combined with the restriction of the Atlantic water advection at the Gibraltar strait due to the global sea level lowering, acted together to increase surface salinities to much higher levels than in the open ocean. In addition, from the lower Pleistocene to Holocene, the interglacial Mediterranean temperatures were rather stable while the glacial Mediterranean temperatures became progressively cooler by about 4°C to 5°C in response to the global climatic deteri-

oration, as evidenced by the development of extensive ice sheets in northern Europe and in the Alps and Pyrenees.

The $\delta^{13}\text{C}$ variations of *G. bulloides* throughout the Pleistocene at Site 975 show that in the West Balearic Basin, as in the global ocean, the glacial periods were generally more productive than the interglacial periods. The detailed examination of the $\delta^{13}\text{C}$ curve shows that the glacial-interglacial transition is often accompanied by a rapid drop (more negative) in $\delta^{13}\text{C}$ values; during full interglacial stages, $\delta^{13}\text{C}$ oscillates between low values and high values that may reach those of glacial stages. This means that in addition to the effect of the global ocean $\delta^{13}\text{C}$ variation, the $\delta^{13}\text{C}$ record in the west Mediterranean registers also specific responses to local changes in the hydrological conditions controlling productivity, mostly the thermohaline stratification of the surface waters.

During periods of high primary production and strong stratification in the surface waters, the upper waters become enriched in ^{13}C because the ^{12}C -depleted CO_2 is preferentially used by phytoplankton; the resulting increased rate of remineralization causes the release of ^{12}C -depleted CO_2 in the underlying waters, which are then up-mixed by homogenization of the water column during the winter convection. As a result, *G. bulloides* that are living in spring blooms where the upper water layers are fertilized by the recycled nutrients, would exhibit low $\delta^{13}\text{C}$ values.

The hypothesis of shoaling pycnocline, related either to sea-level lowering during glacial times or to decreased excess evaporation during sapropel deposition was evoked by Ganssen and Troelstra (1987) and Rohling (1994) to explain the fertilization of surface waters and the enhanced fluxes of export production that is preserved in the sediment at the time of sapropel deposition. The deepening of the pycnocline, which may occur by the decrease of the temperature and/or salinity vertical gradient, would stop the supply of deep nutrients to the surface where oligotrophic conditions prevail.

The sapropel layers were deposited during interglacial stages or warm episodes of glacial stages; a few layers occurred during glacial stages, but at times of transition from cold to warmer conditions. They are mostly characterized by low $\delta^{13}\text{C}$ values of *G. bulloides*, indicative of enhanced nutrient supply to the depth of the pycnocline and thus of high levels of primary production in the surface waters.

The deposition of sapropels at Site 975 was not a regular process since the time span between two sapropels can range between 1 k.y. and 189 k.y. (Table 1). All sapropels are correlated with the maximum values of the 65°N summer insolation curve, and each of them may be ascribed to one insolation cycle (Table 1), following the codification of Laskar (1990). Most of the sapropels identified in the West Balearic Basin are synchronous to the sapropel layers of the eastern Mediterranean; the first sapropel (536) at 1809 ka is contemporaneous of sapropel C6 defined by Verhallen (1987) and the last sapropel (501) at 123 ka is equivalent to sapropel S5 (Ryan, 1972). Sapropels S1, S2, S3, S4, and S8 are lacking at Site 975, but low $\delta^{13}\text{C}$ values of *G. bulloides* at 8 ka, 55 ka, 80 ka, 102 ka, and 217 ka, which are the times of their deposition in the eastern Mediterranean, might indicate increasing rates of organic matter remineralization at subsurface depths in the West Balearic Basin; however, deep ventilation would have been strong enough to prevent the preservation of the sinking particulate organic matter. The recent results obtained in the eastern Mediterranean cores from ODP Leg 160 will make the correlation between the stagnation events in the different parts of the Mediterranean more precise.

CONCLUSIONS

At Site 975, four major periods—Intervals I–IV—have been defined by the amplitude of variations of $\delta^{18}\text{O}$ values. The lower interval boundary at 1.7 Ma occurs above the Pliocene/Pleistocene boundary; the interval boundary at 0.9 Ma, corresponds to a time of signif-

icant ice volume increase in the Northern Hemisphere; the upper interval boundary at 0.42 Ma, is synchronous to the time when the permanent ice sheet in the Northern Hemisphere reached its maximum dimensions. The glacial-interglacial cycles show the typical 100 k.y. eccentricity period after 0.9 Ma and the 40 k.y. obliquity period before 0.9 Ma. The link between the western Mediterranean and the open ocean is clearly demonstrated because the major paleoclimatologic events, as well as the astronomical periodicity, are recorded by the planktonic $\delta^{18}\text{O}$ values.

The specificity of the Mediterranean is revealed by the higher amplitudes of the $\delta^{18}\text{O}$ oscillations at Site 975, compared to those of the open ocean. Starting from the lower Pleistocene, part of this increase is explained by the progressive cooling of the surface waters during the glacial times by 2°C at 0.9 Ma and then again by 2°C at 0.42 Ma. The other part of the $\delta^{18}\text{O}$ increase during glacial times after 0.42 Ma, is better explained by the increase of excess evaporation over freshwater inputs, which resulted in an increase by 2‰ of the surface salinities, rather than by a local additional cooling by 2°C in the West Balearic Basin.

The variations of the $\delta^{13}\text{C}$ values of *G. bulloides* record both the $\delta^{13}\text{C}$ global change, part of which is related to variations of ocean productivity, characterized by high glacial levels and low interglacial levels, and the local modifications of the productivity, which are controlled by the thermohaline stratification of the surface waters.

The sapropel layers were mostly deposited during interglacial episodes where high levels of surface productivity existed. The synchronism of these events with the sapropel deposition in the eastern Mediterranean is verified, but a few layers are not present at the same time in the western and eastern Mediterranean. A precise comparison of the recent results obtained from ODP Legs 160 and 161 is thus necessary to define the interconnections which existed between the western and eastern Mediterranean during the Quaternary.

ACKNOWLEDGMENTS

We thank R. von Grafenstein for stimulating discussions. A special thank-you is addressed to E. de Kaenel for the long and constructive exchanges to obtain a unique coherent chronology based on the nannofossil and oxygen isotope time scales. We are also greatly indebted to the two reviewers who have largely contributed to improve the initial manuscript. Thanks are due to L. Vigliotti for supplemental samples from Hole 975C. Isotopic analyses completed in the U.S. were supported by the USAAC/JOI funding. The isotopic analyses completed in France received the financial support of the Institut National des Sciences de l'Univers of CNRS (INSU grant no. 96 "Géosciences Marines").

REFERENCES

- Bassinot, F.C., Labeyrie, L.D., Vincent, E., Quidelleur, X., Shackleton, N.J., and Lancelot, Y., 1994. The astronomical theory of climate and the age of the Brunhes-Matuyama magnetic reversal. *Earth Planet. Sci. Lett.*, 126:91–108.
- Comas, M.C., Zahn, R., Klaus, A., et al., 1996. *Proc. ODP, Init. Repts.*, 161: College Station, TX (Ocean Drilling Program).
- Craig, H., 1957. Isotopic standards for carbon and oxygen and correction factors for mass-spectrometric analysis of carbon dioxide. *Geochim. Cosmochim. Acta*, 12:133–149.
- , 1965. The measurement of oxygen isotope paleotemperatures. In Tongiorgi, E. (Ed.), *Stable Isotopes in Oceanographic Studies and Paleotemperatures, Spoleto, 1965*: Pisa (Consiglio Nazionale delle Ricerche, Laboratorio di Geologia Nucleare), 1–24.
- Emeis, K.-C., Robertson, A.H.F., Richter, C., et al., 1996. *Proc. ODP, Init. Repts.*, 160: College Station, TX (Ocean Drilling Program).
- Fairbanks, R.G., 1989. A 17,000-year glacio-eustatic sea level record: influence of glacial melting rates on the Younger Dryas event and deep-ocean circulation. *Nature*, 342:637–642.

- Ganssen, G.M., and Troelstra, S.R., 1987. Paleoenvironmental change from stable isotopes in planktonic foraminifera from Eastern Mediterranean sapropels. *Mar. Geol.*, 75:210–218.
- Hilgen, F.J., 1991. Astronomical calibration of Gauss to Matuyama sapropels in the Mediterranean and implication for the geomagnetic polarity time scale. *Earth Planet. Sci. Lett.*, 104:226–244.
- Laskar, J., 1990. The chaotic motion of the solar system: a numerical estimate of the size of the chaotic zones. *Icarus*, 88:266–291.
- Lourens, L.J., Antonarakou, A., Hilgen, F.J., Van Hoof, A.A.M., Vergnaud-Grazzini, C., and Zachariasse, W.J., 1996. Evaluation of the Plio-Pleistocene astronomical timescale. *Paleoceanography*, 11:391–413.
- Pierre, C., in press. The oxygen and carbon isotope distribution in the Mediterranean water masses. *Mar. Geol.*
- Prell, W.L., Imbrie, J., Martinson, D.G., Morley, J.J., Pisias, N.G., Shackleton, N.J., and Streeter, H.F., 1986. Graphic correlation of oxygen isotope stratigraphy: application to the late Quaternary. *Paleoceanography*, 1:137–162.
- Pujol, C., and Vergnaud-Grazzini, C., 1995. Distribution patterns of live planktic foraminifera as related to regional hydrography and productive systems of the Mediterranean Sea. *Mar. Micropaleontol.*, 25:187–217.
- Rohling, E.J., 1994. Review and new aspects concerning the formation of eastern Mediterranean sapropels. *Mar. Geol.*, 122:1–28.
- Ryan, W.B.F., 1972. Stratigraphy of late Quaternary sediments in the Eastern Mediterranean. In Stanley, D.J. (Ed.), *The Mediterranean Sea*: Stroudsburg, PA (Dowden, Hutchison and Ross), 149–169.
- Shackleton, N.J., Berger, A., and Peltier, W.A., 1990. An alternative astronomical calibration of the lower Pleistocene timescale based on ODP Site 677. *Trans. R. Soc. Edinburgh: Earth Sci.*, 81:251–261.
- Tiedemann, R., Sarnthein, M., and Shackleton, N.J., 1994. Astronomic timescale for the Pliocene Atlantic $\delta^{18}\text{O}$ and dust flux records of Ocean Drilling Program Site 659. *Paleoceanography*, 9:619–638.
- Vergnaud Grazzini, C., Saliège, J.F., Urrutiaguer, M.J., and Iannace, A., 1990. Oxygen and carbon isotope stratigraphy of ODP Hole 653A and Site 654: the Pliocene-Pleistocene glacial history recorded in the Tyrrhenian Basin (West Mediterranean). In Kastens, K.A., Mascle, J., et al., *Proc. ODP, Sci. Results*, 107: College Station, TX (Ocean Drilling Program), 361–386.
- Verhallen, P.J.J.M., 1987. Early development of *Bulimina marginata* in relation to paleoenvironmental changes in the Mediterranean. *Proc. K. Ned. Akad. Wetensch.*, B90:161–180.

Date of initial receipt: 31 July 1997

Date of acceptance: 27 February 1998

Ms 161SR-266